Applied Radiation and Isotopes 212 (2024) 111475

Contents lists available at ScienceDirect

Applied Radiation and Isotopes

journal homepage: www.elsevier.com/locate/apradiso

Radioactive sources search method based on multi-robot and Voronoi partition

Dong Yan, Yufeng Xiao *, Shizun Sheng, Zhenyu Ren, Shuang Yang

Special Environment Robot Technology Laboratory, School of Information Engineering, Southwest University of Science and Technology, Mianyang, 621010, China

ARTICLE INFO

Keywords:
Voronoi partition
Multi-robot
Radioactive source localization
Particle filtering

ABSTRACT

In this paper, it is proposed to locate multiple unknown radioactive sources within a certain time limit through particle filtering and Voronoi partitioning. Firstly, with each robot as a Voronoi centroid, the entire area is partitioned. Then, the robots conduct source search concurrently through particle filtering. When all the robots complete the process of one-particle filtering, the iteration ends and the next one begins until the search for the radioactive source is terminated. Finally, experiment is conducted to demonstrate the efficiency and accuracy of the proposed method.

1. Introduction

To locate radioactive sources accurately and promptly is essential for achieving such purposes as nuclear safety, environmental monitoring, and others(Cho and Woo, 2016). In various nuclear facilities such as nuclear power plants or research reactors, the leak of radioactive materials can occur due to natural disasters(Feng et al., 2020). In terms of environmental monitoring, the inadvertent loss of radioactive sources or minerals can endanger the safety of local residents(Jiang, 2009). In case of nuclear accidents or radiological incidents, locating radioactive sources promptly and accurately plays a crucial role in containing radiation and minimizing the exposure to it(Aage, 2003).

The traditional way of responding to nuclear accidents is often troubled by the challenge in conducting rapid search within a large area by a single robot(Chen, 2023). Therefore, it is advantageous to perform this task by applying multiple cooperative robots. For instance, a multi-robot system can be used to accelerate the search operation, particularly when time limit applies. Such a system is robust to various uncertainties like malfunction, non-static environment, and hazardous interference(Queralta et al., 2020).

Currently, research has been conducted worldwide to locate radioactive sources by analyzing the gamma dose rate measured by the nuclear radiation detector mounted on a robot. There are two primary methods used to conduct multi-robot search of radioactive sources: formation search and non-formation search. Formation search involves the intricate coordination and close cooperation among multiple robots, which usually requires synchronization and guidance under a team leader robot to collectively search a designated area. However, this approach is inefficient due to the centralized formation around the leader robot, which poses the risk of collision and the challenge in formation control. In contrast, non-formation source search adopts a distributed strategy that balances autonomy with centralized elements. Each robot defines its own search area independently, which avoids crossing boundaries, thus minimizing the risk of collision and the challenge in formation control. This method is applicable to plan work areas based on the conditions of search in real time, mitigate the global error caused by the inaccuracy of a single leader robot and enabling the robustness to fault. Non-formation search prioritizes robot independence and autonomy, making it applicable to extensive search and in the environments where inter-robot communication is limited. Regarding formation search, Wu (2021) proposed to locate out-of-control nuclear radioactive sources through multi-robot formation. Radioactive source parameter estimation and formation movement can be achieved through distributed formation control and enhanced particle filtering algorithms, which improves the efficiency and accuracy in locating out-of-control radioactive sources. Fan(Fan, 2022) proposed that radioactive source positioning can be achieved for multi-robot formation by using a distributed formation control method and an improved particle filter algorithm based on least squares. In this way, rapid, stable, and precise positioning was enabled in expansive environments. Huo (Ling et al., 2022) proposed a method of collaborative search for unknown radioactive sources through multi-robot information fusion and under an adaptive step-size free energy strategy. On the basis of cognitive difference, the measurement information collected from other

* Corresponding author.
E-mail address: xiaoyf_swit1@163.com (Y. Xiao).

https://doi.org/10.1016/j.apradiso.2024.111475
Received 28 April 2024; Received in revised form 3 July 2024; Accepted 14 August 2024
Available online 17 August 2024
0969-8043/© 2024 Elsevier Ltd. All rights are reserved, including those for text and data mining, AI training, and similar technologies.

robots is selectively fused to estimate the probability distribution of the radioactive source. According to this method, multiple robots move in a fixed formation. Meanwhile, they are coordinated but independent of each other in terms of source estimation and motion control, in addition to coordination. These robots operate only through the data exchange with their neighbors(Ristic et al., 2020; Ristic, 2008).

Regarding the non-formation search, Wiedemann(Wiedemann et al., 2019) used factor graphs and message-passing algorithms to develop a method of multi-robot air source parameter estimation under sparsity constraints, accelerating the process of identifying such source parameters as location and activity. Steiner(Steiner Bourne et al., 2019) proposed to locate a chemical source using a Particle Swarm Optimization (PSO) algorithm with distributed UAVs in urban and suburban environments, thus improving the success rate and efficiency of source positioning. To improve the PSO multi-robot gas source search algorithm, Feng(Feng et al., 2019) focused on how to optimize the performance in source positioning. Cortez(Cortez et al., 2011) presented a decentralized coordination algorithm that allows a group of sensor robots to navigate in a region with non-convex obstacles and perform measurement in the area with the highest probability of "good" information. This approach is reliant on a prior knowledge of known scenarios in the search space or scenarios where the number of areas a team of robots can search is limited when time limit applies. By integrating Voronoi partitioning, global optimization technology, and enhanced navigation functions, this algorithm optimizes the detection by sensors. It also verifies the priority sensing behavior and tendency of collision avoidance. Renzagli(Rahbar and Martinoli, 2020) developed a strategy used to search weak sources with limited communication. With multiple robots moving randomly around a circle, the gradient of a collaboratively estimated signal is measured by using the noise exchange information. According to the method of multi-robot source search, each robot performs estimation independently and shares the source information to determine the optimal control action. However, since each robot makes decision independently, the decision taken by the entire team may not be optimal if the entire team moves in a fixed formation. Park(Park and Oh, 2020) proposed a collaborative multi-robot approach for source search, with the accuracy of source item estimation improved by exchanging sensor measurements with each robot. Each robot then shares and negotiates decisions with the rest of the team until convergence or when the maximum number of iterations is reached. Song(Song et al., 2020) presented a method of weighted Bayesian source term estimation through particle filter and Gaussian fitting in combination. In addition, a Gaussian density function was introduced to fit random samples (particles), thus reducing the bandwidth of communication as required to obtain cognitive differences. Instead of sharing the entire probability map, each robot shares only the mean and covariance of the Gaussian density that can be estimated to measure cognitive differences. In recent years, widespread attention has been paid to the online estimation methods involving mobile sensors for their high flexibility. Sequential estimation is a common strategy explored in such studies (Ji et al., 2022), because a mobile sensor is inadequate to measure an entire area in real time.

2. Related research

It is usually challenging to achieve the collaboration and coordination among multiple robots, and the coverage problem is a clear manifestation of the outcome of such distributed collaboration(Poor, 2015; Zhang et al., 2021; Wei et al., 2021; Wang et al., 2022). When multiple robots are deployed for coverage, each robot has a local map, and the information carried by them differs. Eventually, it must be merged into a global map as a result of the coverage. Due to the limit on communication volume, it is impossible for the robots to share the entire map in real time through communication. Besides, when the number of robots increases, it is inappropriate to adopt a fully connected communication topology(Liu et al., 2019; Yan et al., 2017). Since the robot needs to process a large amount of sensor data (such as laser and vision, etc.), it is also necessary to run coverage algorithm programs, and to communicate and exchange information with other robots. This is undoubtedly a time-consuming process, which makes it difficult to issue the control command in real time. This requires the application of a discrete-time system model that plays the role of a robot. Although the results of using the distributed method are still not necessarily optimal, the whole team can still complete the task successfully when the robot is absent. This illustrates the robustness of the multi-robot system (Xu et al., 2021; Bechlioulis et al., 2019). The description of uncertainty in information through probability can be adapted to various uncertainty models to effectively represent the sensory data collected by noisy sensors. This approach leads to an improved robustness in practice. In terms of the methods used for source positioning, it is assumed in most studies that the relative position of the robots in the initial state is known, thus simplifying the problem(McMahon and Plaku, 2021). In the process of continuous research, this assumption is also rejected. For example, particle filtering is performed to estimate the relative position between robots(McMahon and Plaku, 2023; VasiljevićG et al., 2020). In terms of robustness, fully distributed multi-robot systems outperform single robot or centralized systems(Wang et al., 2014; Ding et al., 2022; Li and Du, 2018; Gao and Zhang, 2022; Abichandani et al., 2023). However, there is a new challenge facing a fully distributed multi-robot system, that is, to reduce various problems such as goal conflicts and area duplication among robots by organizing and coordinating the exploration behavior of multiple robots effectively (Yue et al., 2022; Wang et al., 2017).

Huang(Huang and Wang, 2023) proposed a dynamic partitioning strategy by using Voronoi diagrams. Through partitioning, each robot operates within its own Voronoi partition independently, with no priority order established among the robots. Zhao(Zhao et al., 2023) performed a two-dimensional simulation to analyze the distribution of radiation fields generated by multiple radioactive sources. Then, specific regions were allocated to each robot for further investigation. Xu(Xu et al., 2023) proposed that each agent is able to estimate the probability of a target existing at a given location online according to local probability maps. Subsequently, these local probability maps are fused to determine the posterior probability distribution for target prediction. On this basis, the search path of each agent in the Voronoi cell is flexibly adjusted online to ensure that each agent can be used to conduct search for the target more efficiently. Saha(Saha et al., 2022) introduced the concept of cell centroid Voronoi division, suggesting that this method maximizes the coverage area by ensuring that no coverage holes are created. Therefore, the approach is considered to be robust.

It is challenging to conduct search for and locate multiple radioactive sources. The existing methods focus mainly on single sources, and there are certain limitations on the techniques developed for dealing with multiple sources.

In this paper, a method of multiple unknown sources search is proposed through Voronoi partition and particle filtering. The term "unknown" means that the location, dose intensity and radioactive probability distribution are unknown. Firstly, the entire area of search is divided into several subregions through Voronoi partitioning, with each robot responsible for one subregion. Then, multiple robots execute the particle filter algorithm in parallel within their respective subregion until the exit condition is met. In contrast to the traditional single-robot method, each robot in this algorithm receives radiation from all the sources, with the sum of radiation dose values measured at each point. Due to the characteristics of Voronoi diagram, the distance of a robot from any point within its subregion to its cell center is smaller than that from any point outside it. Due to the inverse square law, the dose value of a radioactive source is inversely proportional to the square of the distance from the source to the robot. When experiment is conducted in larger areas, the dose value of the radioactive source within its own subarea accounts for a relatively significant proportion. The square of distance from the sources outside this sub-region leads to larger values,

Table 1
The definition of symbols used in this paper.

Symbols used in this paper	Symbol meaning
n	Number of robots.
$\{ R_j \}$	The relative position of each robot is a set.
R_x	The x-th robot.
S_n	N-th radioactive source.
P_{rx}	The set of particles dispersed throughout the area by the x-th robot
A	Target area.
M	The number of particles used by each robot.
k	Filter iteration threshold.
$f(p,q)$	The agent's cost function is usually used to measure the movement cost of each robot.
V_i	The Voronoi region of the i-th robot.
$\{C_1,C_2,C_3, \ldots,C_n \}$	A collection of location information for each robot.
C_i	The centers of the Voronoi subregions.
C_i'	Cell center's position after movement
C_j	Other cell centers except C_i
q	Any point in the Voronoi region.
O	An observation point in the Voronoi area.
O'	A new observation point close to p in the Voronoi region.
I_A	CPS(count per second) of observation point A.
A_S	The activity of the radioactive source(Bq).
D	Distance from the radioactive source to the robot(m).
ρ	Detection efficiency of radiation detectors.
S	The effective detection area of the radiation detector(m^2).
(x,y)	Robot position coordinates.
t	The threshold for partition count.
L	Line segment
e_x	Positioning deviation
Iter.	Number of iterations

which reduces the proportion of their dose values within their respective regions. However, this small value should not be disregarded. Meanwhile, applying multiple robots to distributed search can expedite the process of locating radioactive sources. In a large experimental area, this method can be used to efficiently and accurately identify multiple radioactive sources within a time limit. This avoids the possibility of multiple robots repeatedly searching the same area and their collision, thus further accelerating the search process.

To avoid any confusion, Table 1 below lists the definition of all symbols used in this paper.

3. Theory and methods

3.1. Core algorithms and steps for robotic teams to search for multiple radioactive sources

Fig. 1 shows a flowchart of the control algorithm that starts by initializing the Voronoi partition. Meanwhile, particle filtering is performed by the robot team. Once a predetermined threshold value is reached, all the robots complete their search for radioactive sources within their respective regions. Ultimately, the multi-robot distributed search for radioactive sources is completed.

3.2. Measurement model for a single radioactive source

For the dose rate model of a single radioactive source, its activity A_S emits only one photon each time it decays if an isotropic gamma-ray point source exists in a vacuum. At this time, its photon emission rate is 100%. With point A as the observation point, the count rate I_A at point A can be approximately expressed as follows.

$$I_A = \frac{A_S S \rho}{4\pi D_A^2} \tag{1}$$

where A_S represents the activity of the radioactive source, D_A represents the distance from the radioactive source to point A, ρ represents the efficiency of detection by the radiation detector, and S represents the effective detection area of the radiation detector. Obviously, the dose rate of the radioactive source is inversely proportional to the square of the distance between the robot and the radioactive source.

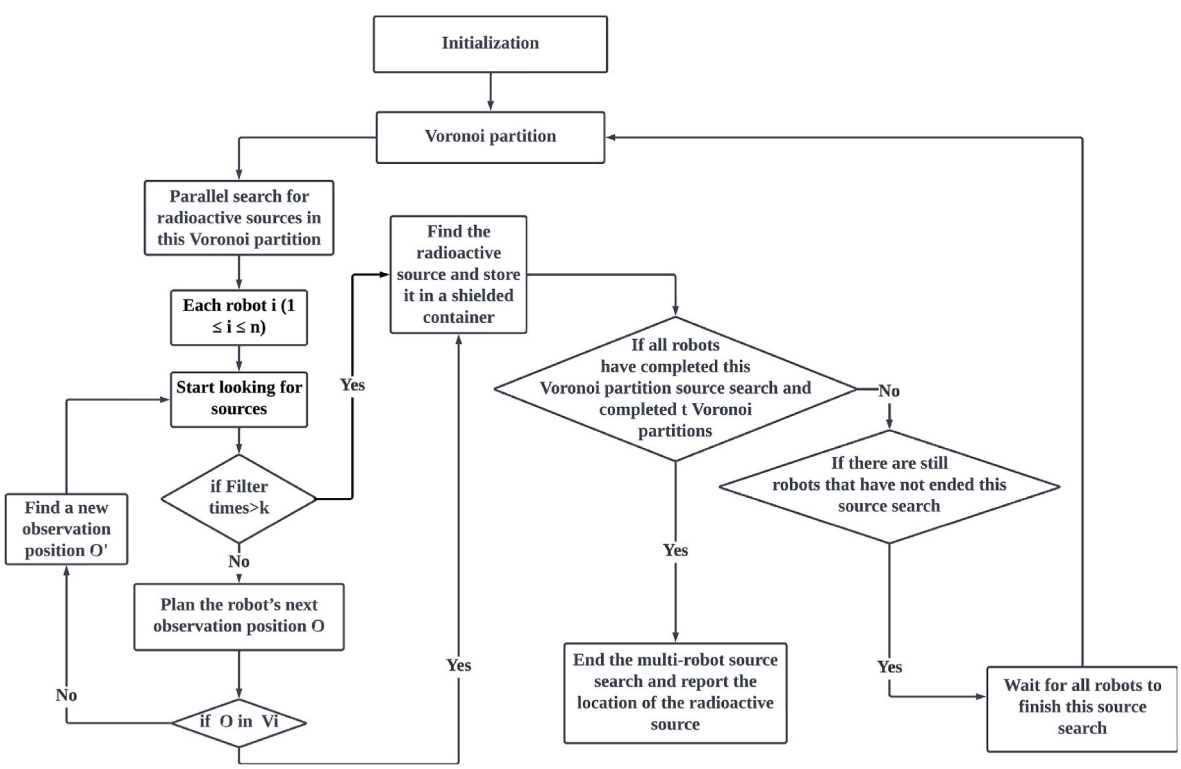

Fig. 1. The flowchart of the control algorithm.

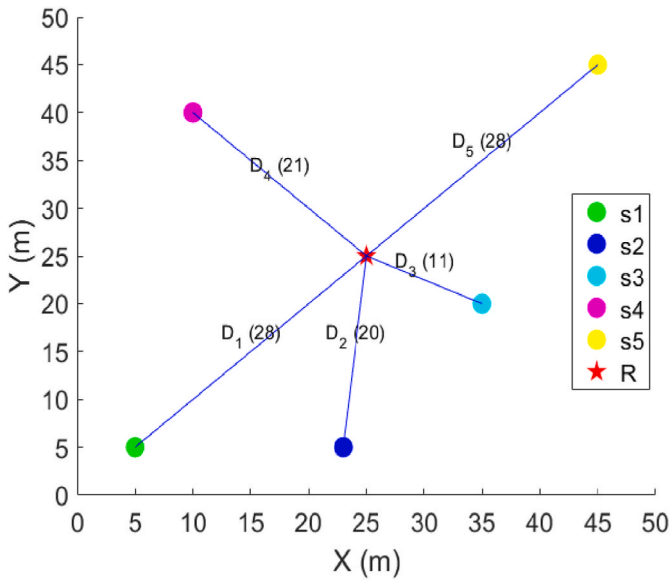

Fig. 2. Schematic diagram of a radiation environment with multiple radioactive sources.

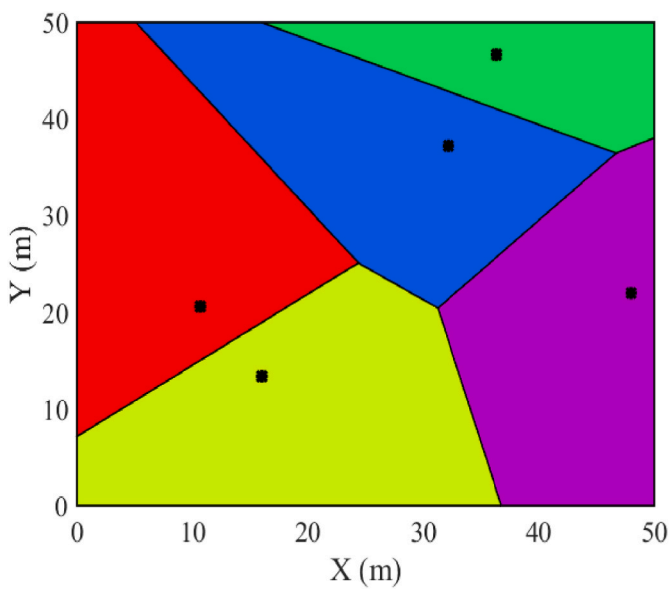

Fig. 3. Voronoi diagram.

3.3. Measurement model for multiple radioactive sources

As shown in Fig. 2, *R* represents the robot, while *s1, s2, s3, s4,* and *s5* represent radioactive sources 1, 2, 3, 4, and 5 respectively. The robot is positioned in a rectangular area that is 50 m long and 50 m wide. There are 5 radioactive sources inside. It is assumed that each of the 5 radioactive sources has its activity value respectively denoted as A_{s1}, A_{s2}, A_{s3}, A_{s4} and A_{s5}. Thus, the distance between the robot and all the sources is respectively denoted as D_1, D_2, D_3, D_4 and D_5. The total radiation count rate absorbed by the robot is denoted as I_{total}, and it can be approximated as follows.

$$I_{total} = \sum_{i=1,j=1}^{i=5,j=5} \frac{A_{si} S \rho}{4\pi D_j^2} \tag{2}$$

3.4. Particle filter algorithm

In essence, the particle filter algorithm is a Bayesian filter algorithm based on the Monte Carlo method. Below is the process followed by it to estimate the probability distribution of the system state.

(1) Initialization: A set of particles are generated randomly, with each particle representing a hypothesis of the system state. Each particle is assigned a weight accordingly.
(2) Prediction: The dynamic model of the system is applied to make prediction for each particle to obtain the assumed state at the next moment.
(3) Updating: The observed data are used to calculate the weight of each particle based on the measurement model, which indicates the degree of fit of the particle to the observed data.
(4) Resampling: Resampling is conducted according to the weight of the particles. The particles with a higher weight are selected with a higher probability, while the particles with a lower weight are removed. This process increases the number of particles with a high weight but decreases the number of particles with a low weight.
(5) State estimation: State estimation requires that the weighted average of the estimated states is calculated using the resampled particles to estimate the current state of the system.
(6) Repeat: The process of prediction, updating, and resampling is repeated. Over time, the distribution of particles is similar to the distribution of the real system state.

3.5. Voronoi partitioning and multi-robot source search

3.5.1. Definition of Voronoi diagram

Suppose *n* robots are randomly distributed in the target area $A \subset R^2$. As the position-related information of multiple robots is $C = \{C_1, C_2, C_3, \ldots, C_n\}$, the Voronoi partition of the target area is expressed as follows.

$$V_i = \{q \in Q | f(C_i, q) \le f(C_j, q), \forall j \ne i, \forall i, j \in n\} \tag{3}$$

V_i refers to the Voronoi region of the i-th robot, *q* represents a point within the Voronoi subregion, and *f(C,q)* refers to the cost function of the robots. The cost function is typically used to calculate the cost of moving the robot from its current position to the target position in the Voronoi diagram.

In this paper, it is assumed that the cost function of each robot is identical and proportional to the distance from the robot to the target point. Therefore, the cost function is expressed as follows.

$$f(C_i, q) = \|C_i - q\|^2 \tag{4}$$

Therefore, the Voronoi partition of the robot team within the target area is expressed as follows.

$$V_i = \{q \in Q \| C_i - q\|^2 \le \|C_j - q\|^2, \forall j \ne i, \forall i, j \in n\} \tag{5}$$

3.5.2. Characteristics of Voronoi diagrams

(1) Each Voronoi polygon contains a cell center point.
(2) The distance from any point within a Voronoi polygon to its cell center is shorter than that to any other cell center.
(3) The points on the boundary of a Voronoi polygon (i.e., points on the common sides of two polygons) have the same distance from the two neighboring cell centers.

Fig. 3 shows a Voronoi diagram divided into five parts. The black dots represent the cell centers of each sub-region, and the different sub-regions have different colors.

Algorithm 1 Multi-Robot Collaboration Source Search Algorithm with Voronoi Partitioning

Input: Number of robots n, Relative positions of each robot$\{R_j\}$, Target area A, activity of radiation source A_s, Number of particles M, Filter iteration threshold k

Output: Position of radiation source

for i=1 *to* n **do**

    Initialize the position of robot i

end for

for i=1 to n **do**

    Determine Voronoi cell center C_i for robot i based on relative positions $\{R_j\}$

end for

repeat

    for i=1 to n **do**

        Initialize particle filter at Voronoi cell center C_i of robot i

        repeat

            Observe CPS and position(x,y) at current location for robot i

            Execute particle filter for robot i

        if the filter estimate converges or filter iterations exceed k **then**

            break

            end if

            Plan next observation position $\boldsymbol{O}$ for robot i

            if $\boldsymbol{O}$ is not in the Voronoi cell of robot i **then**

                Look for new observation position $\boldsymbol{O}'$ in the Voronoi cell of robot i closer to $\boldsymbol{O}$

            end if

        until filter estimate converges or filter iterations exceed k

        if the filter estimate converges or filter iterations exceed k **then**

            Collect radiation source at estimated position for robot i

        end if

    end for

    if all robots finished searching at the current Voronoi region and completed t Voronoi partitions **then**

        Report the position of the radiation source

        Exit

    end if

until all robots finished searching at the current Voronoi region

3.5.3. The generation of the Voronoi diagram

To generate a Voronoi diagram, it is necessary to construct a Delaunay triangulation with its dual elements at first. Then, the circumcenter of each triangle is located and the circumcenters of adjacent triangles are connected to form a network of polygons. In this context, the vertices of each triangle are treated as the cell centers in the Voronoi diagram. By using this method, the Voronoi diagram is effectively generated.

3.5.4. Principle of multi-robot partition source-searching

This is an algorithmic process in which multi-robot collaborative source search is conducted through Voronoi partitioning. Below is a

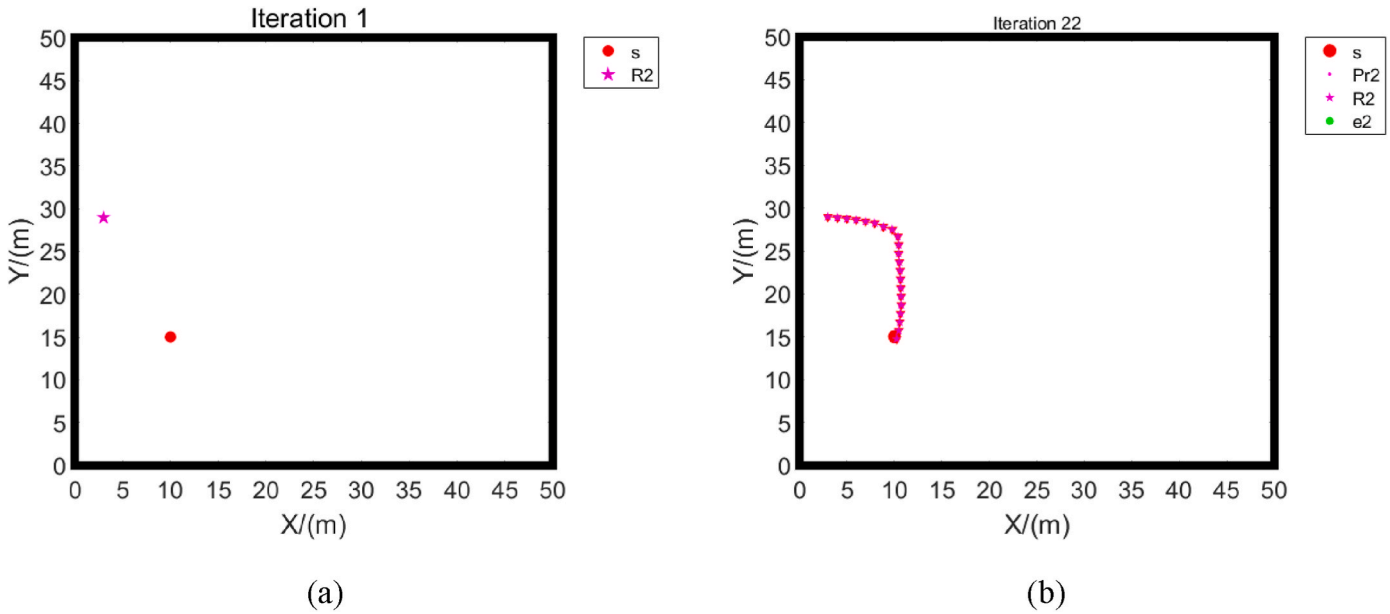

Fig. 4. The process of one robot searching for one radioactive source.

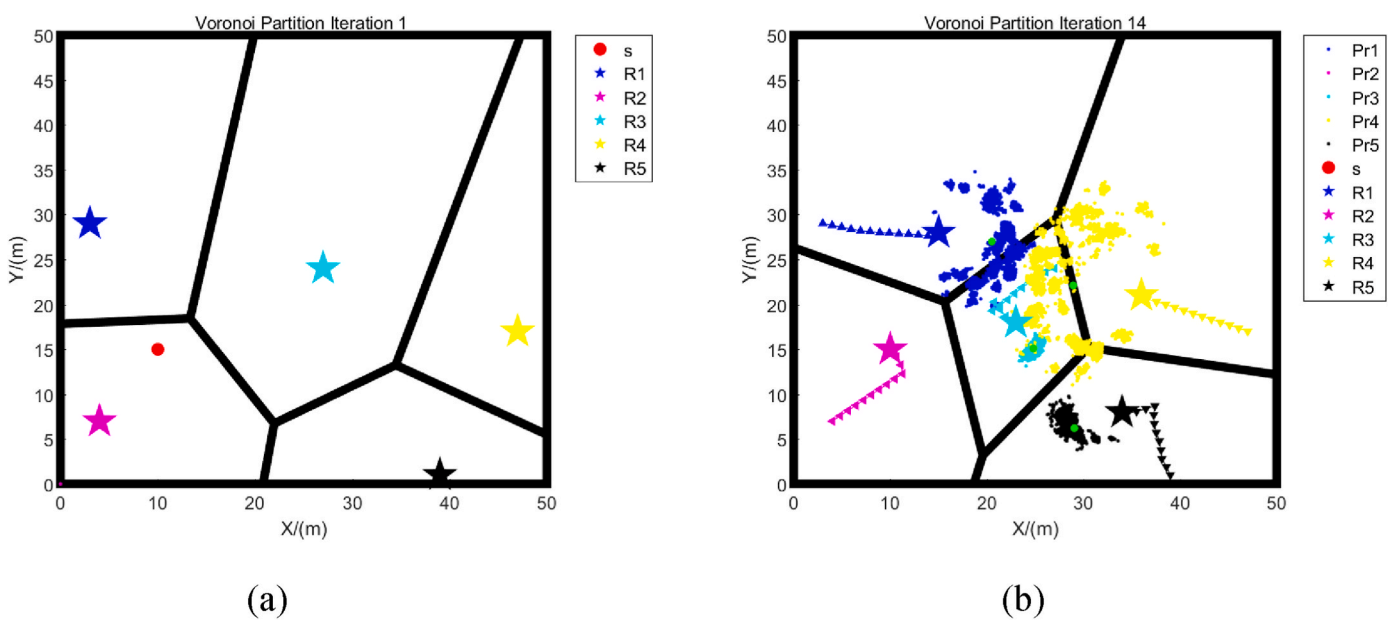

Fig. 5. The process of five robots searching for one radioactive source.

step-by-step explanation of this process.

1. Initialization of n robot positions: n robots are deployed at suitable locations within the search area, either randomly or in a predetermined position.
2. Voronoi partition: Each robot receives the information about relative position through communication, calculates its corresponding Voronoi partition on this basis, and sets the cell center of the Voronoi partition.
3. Parallel source search for this Voronoi partition.
   a) For each robot i ($1 \leq i \leq n$), a particle filter is initialized at the center position of the i-th Voronoi partition.
   b) Source search is conducted by observing the current CPS(counts per second) and position(x, y) as a form of measurement for filtering. Particle filtering is performed to update the weight and state of particles.
   c) It is determined whether the filter estimate satisfies the convergence condition or if the number of filtering exceeds the set threshold k. If satisfied, the algorithm proceeds to Step f; otherwise, it proceeds to Step d.
   d) The next observational position O of the robot is planned according to the filtered estimate.
   e) According to Corollary 1 in appendices A, if the observational position O falls outside the i-th Voronoi partition, the coordinates of the cell center point are referred to as C_i, which can be expressed as $C_i = (x_i, y_i)$. Therefore, it can be expressed as follows.

$$\|C_i - O\|^2 \geq \|C_j - O\|^2 \tag{6}$$

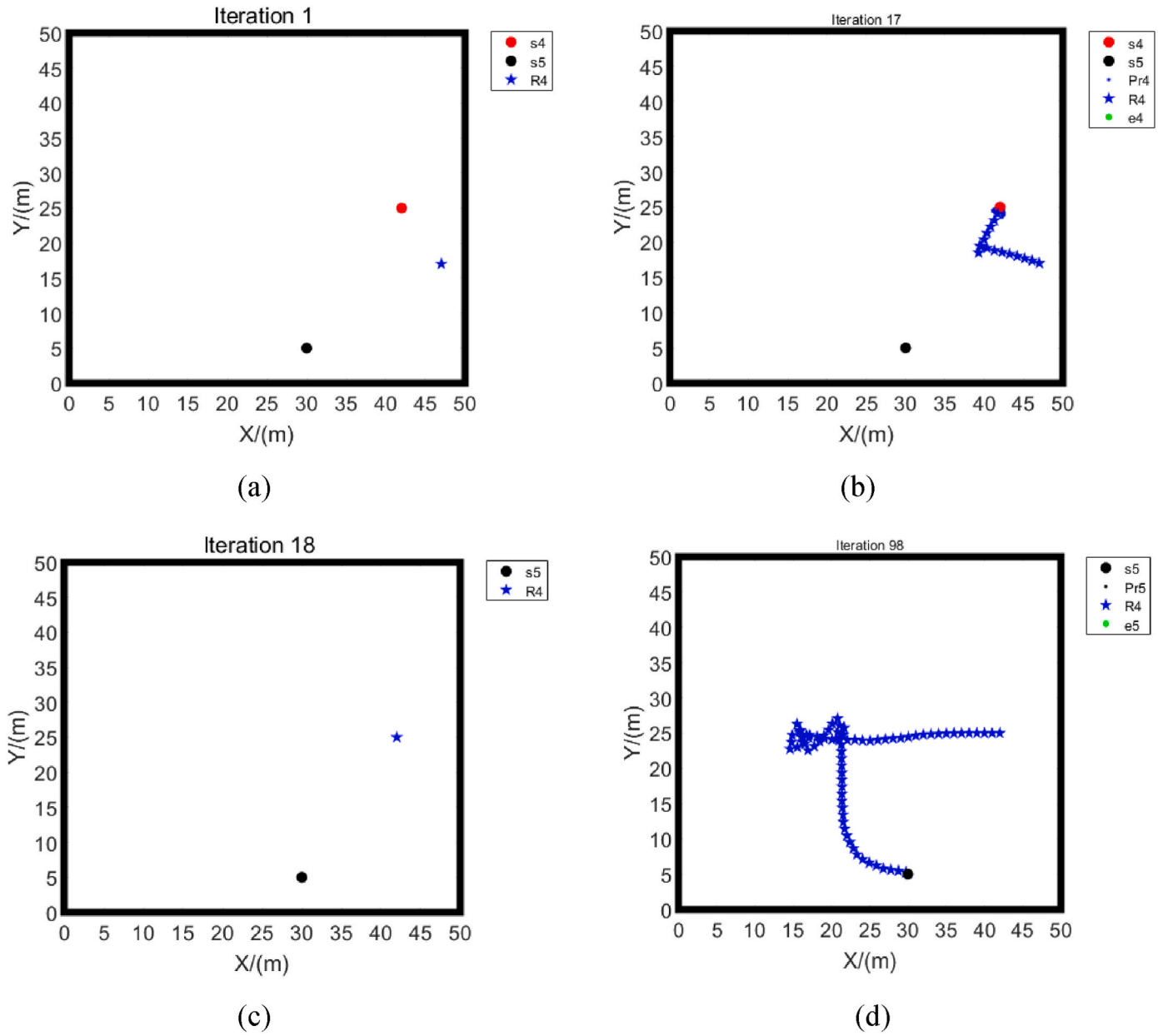

Fig. 6. The process of one robot searching for two radioactive sources.

In other words, if the distance from Position O to the generating point C_i exceeds that to all other generating points C_j, with the generating point C_i of the i-th partition excluded, then Position O is outside the i-th Voronoi partition. Then, a new observational position O' is searched for when O' falls within the i-th Voronoi partition and is close to O. Then, it proceeds to Step b.

f) If the estimation by the filter satisfies the convergence condition, it indicates that the radioactive source has been located and stored in a shielded container. Then, the algorithm proceeds to Step 4. If the number of filtering iterations exceeds k, it indicates that the radioactive source has not been located. In this case, it proceeds to Step 4 as well.

4. If all the robots have completed source search in their respective Voronoi partition and have accomplished t Voronoi partitions, the process of multi-robot source search is terminated, and the location of the radioactive source is reported. If there are some robots failing to complete source search, the process is suspended until all the robots have completed source search. Then, the algorithm reverts to Step 2. When the robots in n Voronoi partitions complete source search in a specific area, the Voronoi partition of the source search area can be re-implemented according to the current position of the robots in each partition as the new cell centers. See Corollary 2 in the appendices Afor details.

This algorithm relies on multi-robot collaboration to simultaneously search for radioactive sources within Voronoi partitions and estimate their locations through particle filtering. It adjusts the observational position of the robots in real time, enabling the efficient and accurate positioning of the radioactive sources.

3.6. Pseudocode for combining Voronoi partitioning with multiple robots

Voronoi partitioning and particle filtering algorithms are the core algorithms applied in this paper. Below is the pseudocode of the

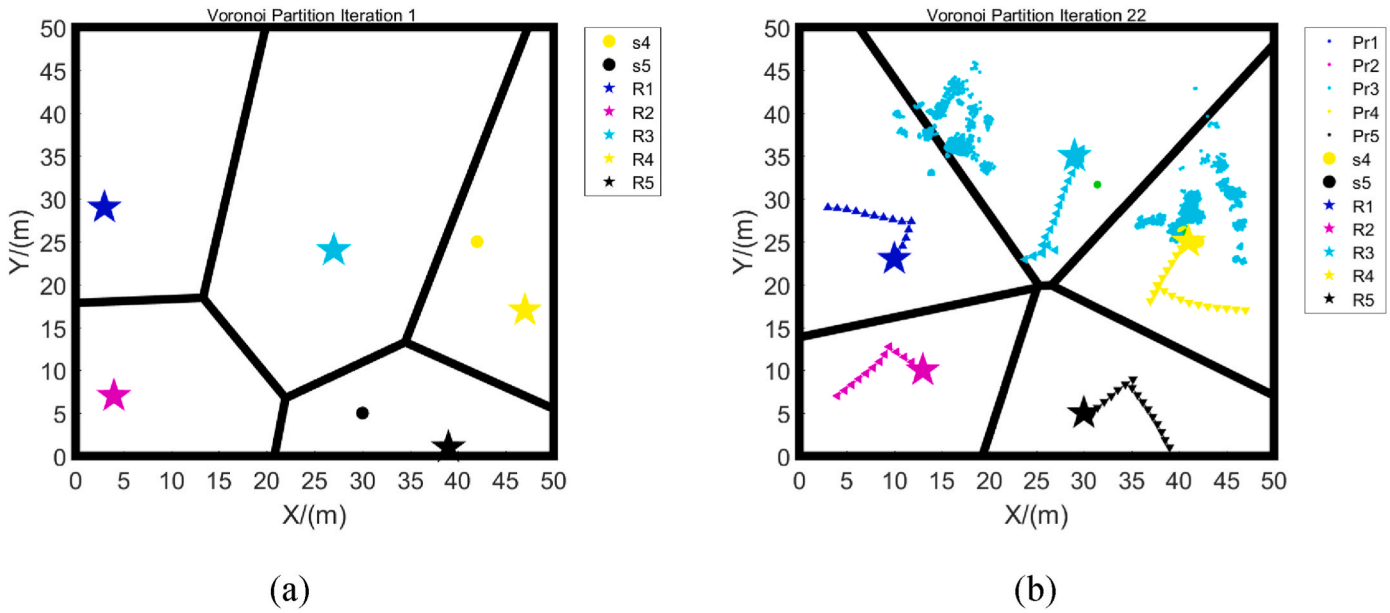

Fig. 7. The process of five robots searching for two radioactive sources.

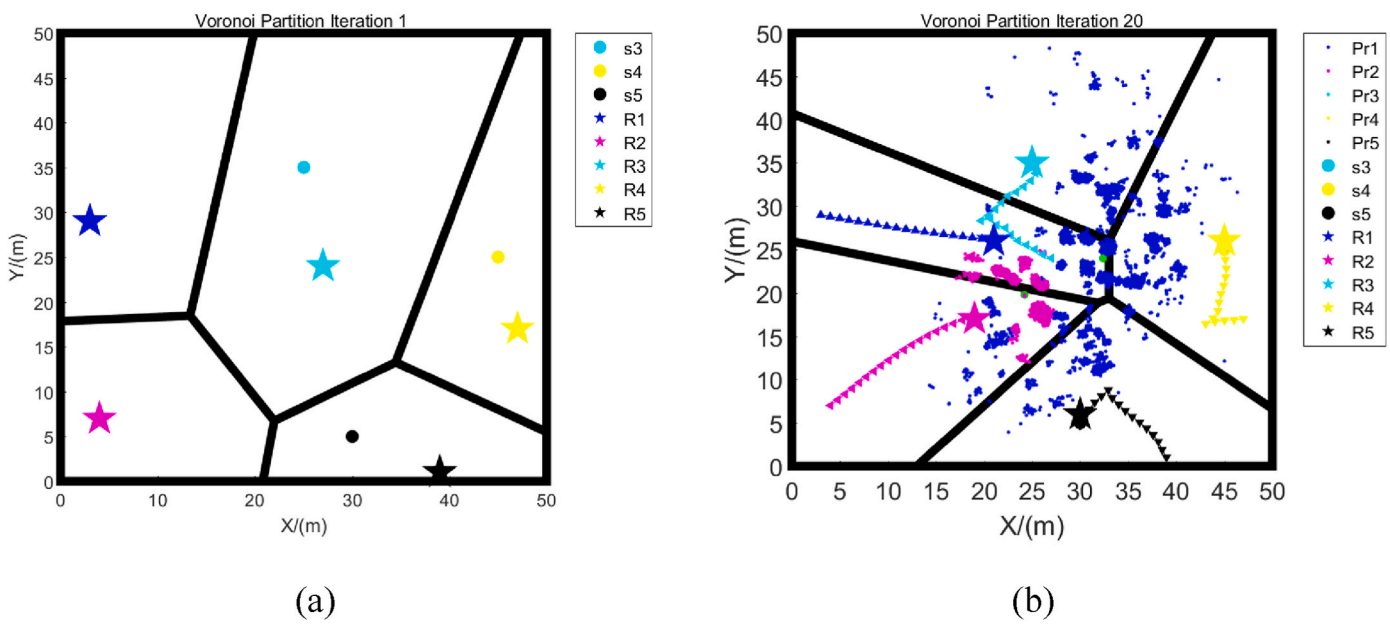

Fig. 8. The process of five robots searching for three radioactive sources.

algorithm that integrates them to accomplish multi-robot source search.

Algorithm 1. Multi-Robot Collaboration Source Search Algorithm with Voronoi Partitioning

4. Results and analysis of simulation experiments

4.1. Experimental arrangements and objectives

In this study, a series of experiments are conducted. Firstly, comparative experiments are conducted between 1V1 and 5V1 configurations, and then between 1V2 and 5V2, so as to evaluate the efficiency of source search comparatively between using a single robot and using multiple robots. With the use of 5 robots, the number of radioactive sources increases from 2 to 6 for assessing the stability and efficiency of the multi-robot source search algorithm. In this algorithm, '1V1' means one robot searches for one radioactive source, '5V1' means five robots search for one radioactive source, and so forth. This experimental design enables a comprehensive evaluation of the level of search efficiency and the performance of multiple robots when the number of radioactive sources varies. By increasing the number of radioactive sources progressively, it is possible to observe how the performance of the robot team in dealing with more complex tasks varies. This provides insights into the potential applicability of multi-robot collaboration in the search conducted for multiple sources.

4.2. Experimental scenes and experimental conditions

Algorithm validation is performed on a computer equipped with an AMD Ryzen 7 5800H with Radeon Graphics 3.20 GHz processor. The software adopted to serve this purpose is Matlab R2022a. The rules of

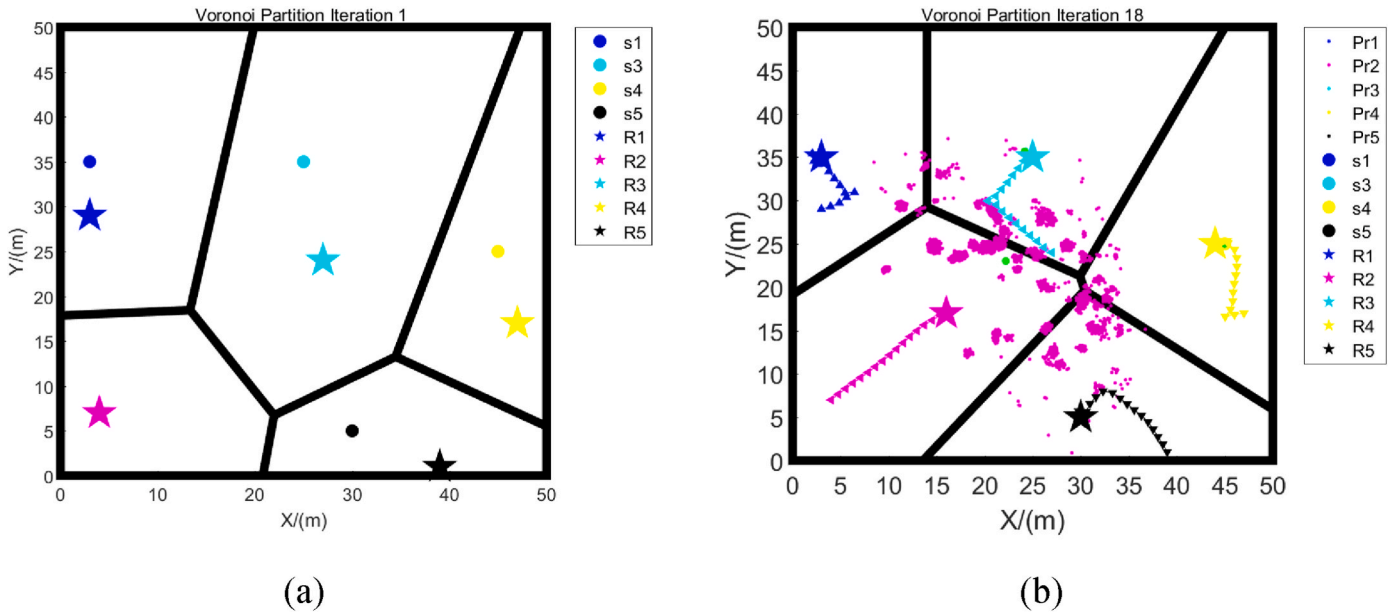

Fig. 9. The process of five robots searching for four radioactive sources.

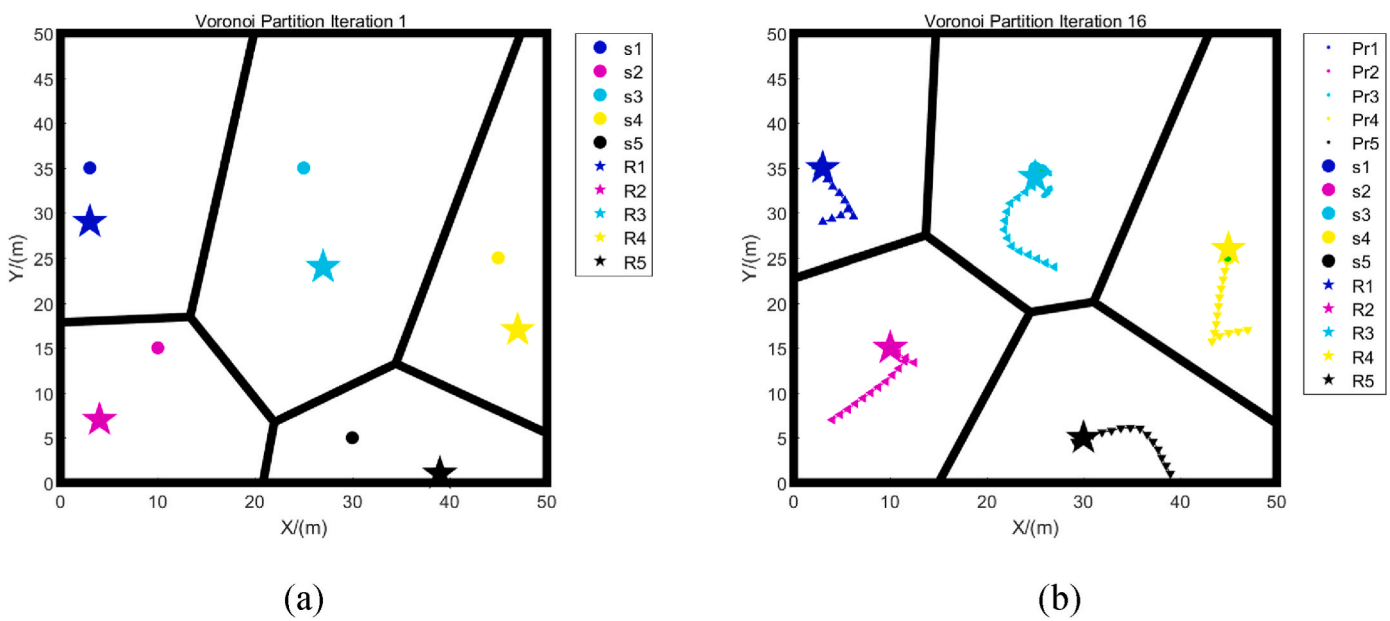

Fig. 10. The process of five robots searching for five radioactive sources.

generation for experimental parameters in the following groups are detailed as follows.

(1) Generation of radioactive source positions: The positions of 1, 2, 3, 4, 5, and 6 radioactive sources are generated randomly within the experimental area sized 50m × 50m to ensure that the sources remain within the boundaries of the area.
(2) Generation of activity: An activity range of 20–80 (unit:MBq) is selected and 10 different activities (43,25,30,36,49,57,62, 78,52,31) (unit:MBq) are generated randomly within the range.
(3) Generation of the initial position of the robot: The initial positions of 5 robots are randomly generated within the experimental area, which prevents overlap or proximity to the position of the radioactive source.

Complying with these rules ensures random distribution for the position of radioactive source, activity, and the robot's initial position in the experiment. Through a combination of different activities and positions of the radioactive source, the reliability of the experimental results is enhanced.

The entire area is partitioned into 5 sub-areas using Voronoi diagrams. The position of each robot corresponds to the cell center of its respective subregion. The five robots activate particle filters simultaneously to search for radioactive sources.

When the distance between the robot and the estimated radioactive source is less than 1 m, the radioactive source is considered as "found". In the following figures including Figs. 4–12, "P_{rx}" represents the set of particles distributed by the x-th robot across the area, and each particle set corresponds to the particles distributed by each robot across the area. In this algorithm, each robot is programmed to distribute 5000 particles

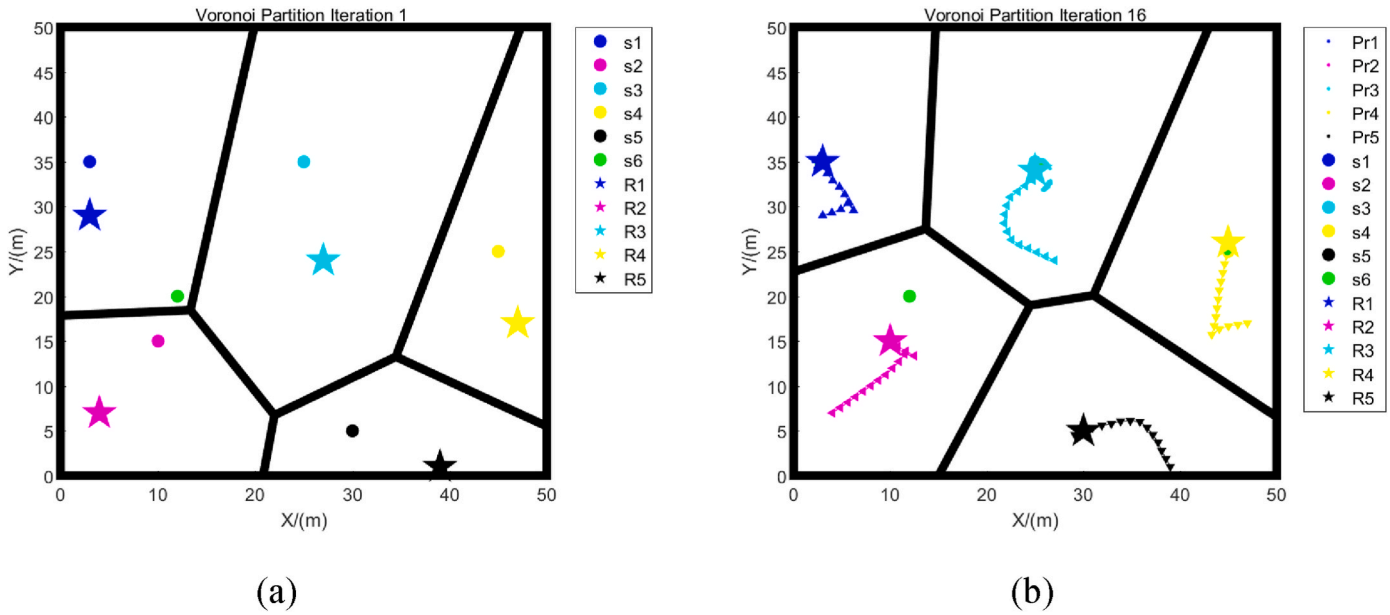

Fig. 11. The process of five robots searching for six radioactive sources.

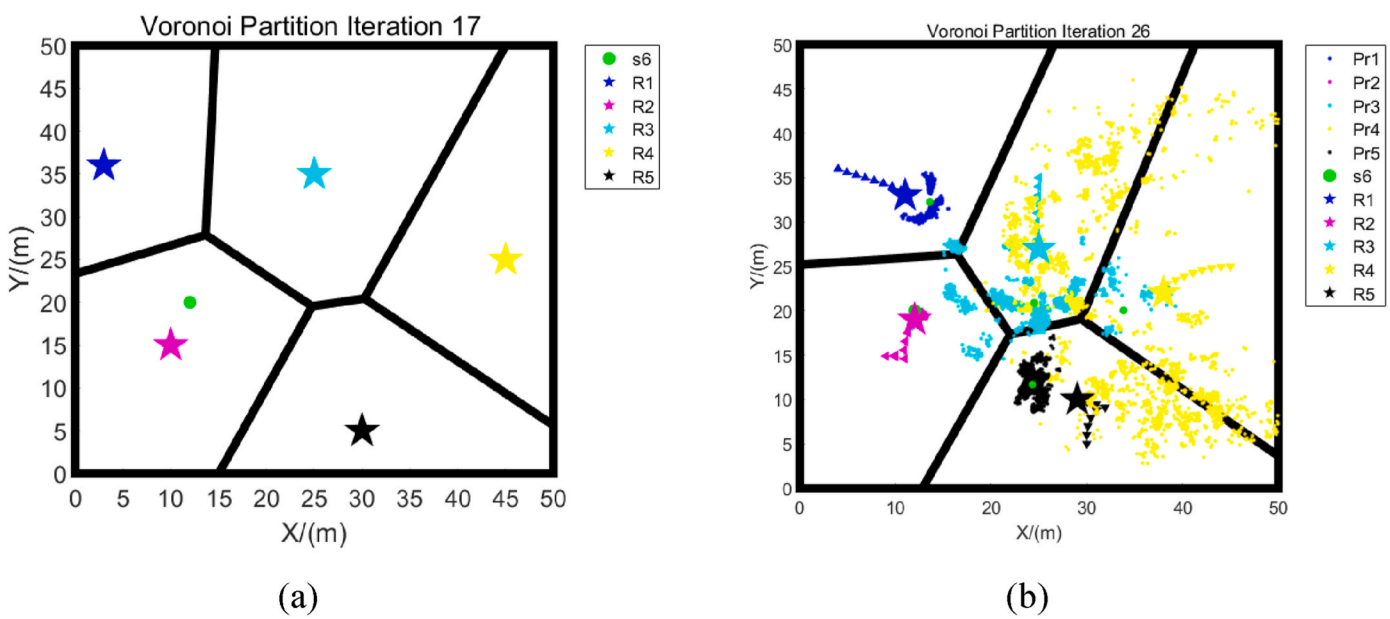

Fig. 12. The process of five robots searching for the sixth radioactive source.

Table 2
Comparison of experimental parameters.

Experiment serial number	$S_{(x,y)}$	5V1	1V1	5V1	1V1	5V1	1V1
		e/(m)		Success		Iter.	
1	(10,15)	0.3	0.8	Yes	Yes	14	22
2	(15,5)	0.5	0.9	Yes	Yes	10	19
3	(0,15)	0.5	0.9	Yes	Yes	12	18
4	(50,50)	0.6	0.7	Yes	Yes	10	22
5	(45,25)	0.4	0.9	Yes	Yes	7	12
6	(45,35)	0.6	0.8	Yes	Yes	9	18
7	(30,50)	0.5	0.7	Yes	Yes	6	13
8	(30,45)	0.5	0.9	Yes	Yes	14	30
9	(25,30)	0.3	0.9	Yes	Yes	7	12
10	(10,35)	0.5	0.6	Yes	Yes	8	17

across the area, resulting in a total of 25000 particles. Additionally, "R_x" represents the x-th robot, and "S_n" represents the n-th radioactive source.

4.3. 1V1

Robot *R2* is deployed in a rectangular area that is 50 m long and 50 m wide, and a radioactive source *s* is placed within this area. Then, Robot *R2* is used to search for the radioactive source by activating a single-source particle filter.

The coordinate of the real radioactive source is (10, 15), and the initial position of the robot is (3, 29), as shown in Fig. 4(a). After 22 iterations, the robot ends up at the coordinate (10.8, 14.9). The error at this time is defined as the Euclidean distance between the termination position of the robot and the coordinate of the real radioactive source. Therefore, Robot *R2* conducts search for the radioactive source with an approximate error of approximately 0.8 m, as shown in Fig. 4(b).

Table 3
Comparison of experimental parameters.

Experiment serial number	S (x,y)	5V2	1V2	5V2	1V2	5V2	1V2
		e/(m)		Success		Iter.	
1	s4 (42,25) s5(30,5)	0.3 0.4	0.8 0.9	Yes	Yes	22	98
2	s4(15,5) s5 (16,25)	0.2 0.4	0.6 0.6	Yes	Yes	19	90
3	s4(0,15) s5(32,5)	0.5 0.2	0.8 0.9	Yes	Yes	20	87
4	s4 (50,50) s5 (30,25)	0.5 0.6	none	Yes	No	16	none
5	s4 (45,25) s5 (10,35)	0.5 0.4	none	Yes	No	18	none
6	s4 (45,35) s5 (30,35)	0.8 0.6	none	Yes	No	17	none
7	s4 (30,50) s5(40,2)	0.4 0.4	0.8 0.8	Yes	Yes	15	88
8	s4 (30,45) s5 (45,40)	0.3 0.4	none	Yes	No	22	none
9	s4 (25,30) s5(36,8)	0.6 0.4	0.8 0.8	Yes	Yes	26	95
10	s4 (10,35) s5 (45,20)	0.5 0.2	0.8 0.9	Yes	Yes	22	90

4.4. 5V1

As shown in Fig. 5(a), there are five robots and one radioactive source. The Voronoi partition is updated in real time as the robot team moves. As the boundaries and partition patterns evolve, each robot stays within its designated partition. Since each robot moves forward 1 m per update, the changes in the Voronoi partition are insignificant each time. Therefore, the initial and final partitions are highlighted to illustrate this evolution. It is evident that the particles continue to converge, with the particle set of Robot 2 eventually converging near the radioactive source. Different robot particle sets converge to varying degrees, and those of the robots not searching for the source converge to a lesser extent.

As shown in Fig. 5(b), Robot 2 searches for the radioactive source with an error of approximately 0.3 m after 14 times of partition.

In Table 2, the number of iterations, errors, and successes are compared between the single-robot search for a radioactive source and the five-robot search for a radioactive source. Additionally, simulation experiment is performed ten times, and data analysis is conducted by adjusting the location and activity of the radioactive source in each experiment. In Tables 2 and 3 below, "Success" denotes success, "Iter." denotes the number of iterations, "e" denotes positioning deviation after successful source search, and "none" denotes an unsuccessful source search without data.

Statistically, the experimental error in the search for a single radioactive source by five robots is less significant compared to the search by a single robot. It is implied that the collaborative search by multiple robots is effective in reducing experimental errors. In the case of 5V1, each of the five robots uses 5000 particles. By contrast, only one robot uses 5000 particles in the case of 1V1. Experience shows that the accuracy of particle filtering improves with an increase in the number of particles within a specified range. In an area of the same size, 5V1 uses more particles than 1V1, which enhances the accuracy of estimation.

Moreover, since both strategies aim to locate a single radioactive source within the same area, there is almost no variation in success rate. However, 5V1 requires fewer iterations than 1V1, which indicates that collaborative multi-robot search for radioactive sources can expedite the search process relative to single-robot search that is less efficient. This is attributed to the faster search process by the multi-robot system through Voronoi partitioning. Each robot moves towards the nearest radioactive source efficiently within its designated subregion, thus eliminating the need to search the entire area. As a result, there is a decrease in the number of iterations required to search for radioactive sources across the area.

4.5. 1V2

As shown in Fig. 6(a), Robot *R4* is randomly positioned at (46, 16) within a rectangular area measuring 50 m in length and width. Subsequently, two radioactive sources, *s4* at (42, 25) and *s5* at (30, 5), are also randomly placed within the same area.

According to Fig. 6(b), *R4* locates the radioactive source *s4* successfully after 17 partitions. It then stores *s4* and proceeds to search for the next one. As illustrated in Fig. 6(d), *R4* successfully locates *s5* on the 98th partition.

4.6. 5V2

Similarly, after 22 partitions, *R4* searches *s4* with an error of about 0.3 m, and *R5* searches *s5* with an error of about 0.4 m, as shown in Fig. 7.

According to Table 3, the performance of a single robot searching for

Table 5
Positioning deviation of each radioactive source.

Experiment	e_1 / (m)	e_2/ (m)	e_3/ (m)	e_4/ (m)	e_5 / (m)	e_6/ (m)	Average_e/ (m)
5V3	/	/	0.4	0.3	0.3	/	0.33
5V4	0.6	/	0.5	0.6	0.4	/	0.53
5V5	0.4	0.8	0.8	0.7	0.6	/	0.66
5V6	0.9	0.9	0.9	0.8	0.8	0.9	0.85

Table 6
Statistics on the number of iterations.

Experiment	5V3	5V4	5V5	5V6
Iter.	20	18	16	26

Table 4
The locations of radioactive sources.

Experiment	*S1* (x,y)	*S2* (x,y)	*S3* (x,y)	*S4* (x,y)	*S5* (x,y)	*S6* (x,y)	Corresponding figure
5V3	/	/	(25,35)	(45,25)	(30,5)	/	Fig. 8
5V4	(3,35)	/	(25,35)	(45,25)	(30,5)	/	Fig. 9
5V5	(3,35)	(10,15)	(25,35)	(45,25)	(30,5)	/	Fig. 10
5V6	(3,35)	(10,15)	(25,35)	(45,25)	(30,5)	(12,20)	Figs. 11 and 12

("/" indicates that the source does not exist.)

two radioactive sources is compared with that of five robots searching for the same sources. Additionally, simulation experiment is conducted ten times, with the locations and activity of the radioactive sources changed in each experiment to perform data analysis. To control the variables, the activities of radioactive sources within the same experimental group are kept consistent, while those in different groups are changed and randomly determined.

Statistically, the experimental error of five robots searching for two radioactive sources is less significant than that of one robot searching for these two radioactive sources. It is demonstrated that experimental error can be reduced by the collaborative search by multiple robots for radioactive sources. Moreover, the success rate is higher when five robots search for two radioactive sources than when one robot searches for these two radioactive sources. In case that the search by a single robot fails, multiple robots can complete the search collectively. Additionally, the average number of iterations is lower when five robots search for two radioactive sources than when one robot searches for these two radioactive sources. This illustrates that multi-robot search locates radioactive sources faster than single robot search that is less efficient.

These findings are consistent with the results of comparative experiment on 5V1 and 1V1. Furthermore, it is possible that the fixed step size of 1 m in each iteration increases the cost of a single robot finding the second radioactive source in 1V2. This requires a large number of iterations for effective search.

As revealed by the above comparative experiments, the multi-robot search for multiple radioactive sources is advantageous in reducing experimental error, improving success rate, and minimizing the number of iterations.

4.7. 5 Robots are searching for more quantity radioactive sources

In the following experiments, no change is made to the initial arrangement after multiple robots are randomly deployed. The position of radioactive sources is determined in a uniform and random way for each experiment, as shown in Table 4. This table details the position of the respective radioactive sources in each experimental set. To control the variables, the activities of radioactive sources within the same experimental group are kept consistent, while those in different groups are changed and randomly determined.

4.7.1. 5V3

After 20 partitions, *R3* searches for *s3*, *R4* searched for *s4*, and *R5* searched for *s5*, as shown in Fig. 8. The phenomenon of particle concentration areas is depicted in the figure. This can be understood as the insufficient convergence of multiple robots when the particle filter algorithm is executed. When one of the robots searches for the radioactive source and meets the end condition, the other robots have not completed the search for the radioactive source yet. The robot may continue executing the algorithm because it has not met the convergence condition yet, which causes the failure in convergence of particle collection (the same applies below).

4.7.2. 5V4

After 18 partitions, *R1* searches for *s1*, *R3* searches for *s3*, *R4* searches for *s4*, and *R5* searches for *s5*, as shown in Fig. 9.

4.7.3. 5V5

After 16 partitions, each robot searches for the radioactive source, as shown in Fig. 10.

4.7.4. 5V6

After 16 partitions, each robot searches for radioactive sources 1, 2, 3, 4, and 5. However, *s6* is not searched for, as shown in Fig. 11.

In the next phase, the located sources are processed and stored, while the remaining ones that are not discovered are searched for.

After an additional 10 partitions, *R2* succeeds in searching for the remaining *s6*, as shown in Fig. 12. In total, the five robots complete the search for all the six radioactive sources in 26 partitions.

Table 5 presents the data on positioning deviation for each radioactive source, while Table 6 details the data on iteration for each experiment.

("/" in Table 5 represents no data, "e_x" represents the positioning deviation of the x-th radioactive source, "Average_e" represents the mean value obtained by adding the deviation data in each row and dividing by the number of non-null values, and "Iter." in Table 6 represents the number of iterations.)

From above, it can be seen clearly that each team of robots can effectively search for varying numbers of radioactive sources distributed across the region after a certain number of iterations, which illustrates the effectiveness and robustness of the multi-robot source search method based on Voronoi partitioning.

5. Conclusions and future work

In this paper, a solution is proposed to locate multiple unknown radioactive sources rapidly in case of nuclear emergency. It is also explored how to integrate the distributed robotic teams based on Voronoi partitioning with the particle filtering techniques. This distributed search strategy is validated through simulation experiment to demonstrate the applicability of the proposed algorithm.

In our future research, multiple robots and sources will be used to verify the proposed algorithm in real-world conditions. The multiple radioactive source search algorithm will be optimized to enhance both efficiency and accuracy. Additionally, the collaborative mechanisms of multi-robot teams will be explored, including path planning, information sharing, and task assignment. It is equally crucial to evaluate the algorithm for its applicability in complex and dynamic environments, such as that with various sources of interference. In this way, the robustness and practicality of the algorithm are enhanced.

CRediT authorship contribution statement

Dong Yan: Writing – original draft, Software, Investigation, Data curation. **Yufeng Xiao:** Writing – review & editing, Supervision, Conceptualization. **Shizun Sheng:** Validation, Investigation. **Zhenyu Ren:** Investigation, Formal analysis. **Shuang Yang:** Writing – review & editing, Visualization, Validation.

Declaration of competing interest

The authors declare that they have no known competing financial interests or personal relationships that could have appeared to influence the work reported in this paper.

Data availability

The data that has been used is confidential.

Acknowledgments

This research was funded by the National Natural Science Foundation of China (No.12175187).

Appendices A.

Corollary to Voronoi diagram

Corollary 1: The cell center C_i of a certain partition. After the robot R in the partition moves from the cell center to Point P, the robot crosses the boundary if C_i and the neighbor cell center C_j satisfy $||C_i - P||^2 > ||C_j - P||^2$. $(i \neq j)$

Proof:

Assume that Point q is in a polygon in the Voronoi partition. The cell center of the polygon is denoted as C_i, and the cell centers of other polygons are denoted as C_1, C_2, …, and C_j, respectively. According to the definition of the Voronoi partition, the distance from Point q to Point C_i is in no excess of that from Point q to any other point denoted as C_j. Suppose there exists C_j. Thus, the distance from q to C_j is shorter than the distance from q to C_i. Mathematically, this is expressed as follows.

$$\|C_j - q\|^2 < \|C_i - q\|^2 \tag{A.1}$$

Construction of a contradiction: The line between q and C_j is considered. Since q is in the Voronoi polygon of C_i, the distance from q to C_i is supposed not to exceed the distance from P to C_j. This contradicts the hypothesis.

Conclusion: Therefore, no such C_j exists. For any j(i≠j), the following formula applies.

$$\|C_j - q\|^2 \geq \|C_i - q\|^2 \tag{A.2}$$

That is to say, a point in a Voronoi polygon is closer to the center of the polygon than to that of other polygons. The proof is completed.

Corollary 2: Once the robots in n Voronoi partitions complete source search in a specific area, the Voronoi partition of the source searching area can be reconstructed according to the current position of each robot in each partition as the unit center.

Proof:

The necessary and sufficient condition for Voronoi partitioning is that if a point q is in the Voronoi region of a certain cell center C_i, then for all the other cell centers denoted as C_j, the distance from q to C_i must be shorter than the distance to C_j. Since the robot is positioned at the cell center of the Voronoi partition, the cell center represents the position of the robot. It is proven by demonstrating that the new partition still satisfies the necessary and sufficient conditions of a Voronoi partition when any point q moves with the cell center within the original cell center.

Assume that Point q is in the Voronoi region of the cell center C_i, which means the distance from q to C_i is shorter than the distance to all other cell centers. Now it is necessary to consider the situation after C_i has moved to C_i'.

(1) If the distance from q to C_i' is shorter than the distance to all other cell centers, then q is still in the Voronoi region of C_i' because it is closer to C_i' than to other cell centers.
(2) If the distance from q to C_i' exceeds the distance to all other cell centers but is shorter than the distance to C_i, then q is still in the Voronoi region of C_i. Since C_i has moved, q remains closer to C_i than to other cells.
(3) If the distance from q to C_i' exceeds the distance to all other cell centers and the distance to C_i, then q is no longer in the Voronoi region of C_i. It is assigned to the nearest cell center. The distance from q to C_i' exceeds that to all other cell centers, and q is still closer to C_i' than to other cell centers. Therefore, q is assigned to C_i'.

To sum up, the sufficient and necessary conditions of Voronoi partition are still satisfied after C_i moves to C_i'. Thus, the proof is completed.

References

Aage, H.K., 2003. Korsbech U. Search for lost or orphan radioactive sources based on NaI gamma spectrometry. Appl. Radiat. Isot. 58 (1), 103–113.

Abichandani, P., Lobo, D., Muralidharan, M., et al., 2023. Distributed motion planning for multiple quadrotors in the presence of wind gusts. Drones.

Bechlioulis, C.P., Giagkas, F., Karras, G.C., et al., 2019. Robust Formation control for multiple underwater vehicles. Frontiers in Robotics and AI 6.

Chen, et al., 2023. Overview of multi-robot collaborative SLAM from the perspective of data fusion. Machines 11, 653. https://doi.org/10.3390/machines11060653.

Cho, H.S., Woo, T.H., 2016. Mechanical analysis of flying robot for nuclear safety and security control by radiological monitoring. Ann. Nucl. Energy 94, 138–143.

Cortez, R.A., Fierro, R., Wood, J., 2011. Prioritized sensor detection for environmental mapping: theory and experiments. J. Intell. Rob. Syst. 63 (3–4), 481–501.

Ding, S., Aoyama, H., Lin, D., 2022. Combining Multiagent Reinforcement Learning and Search Method for Drone Delivery on a Non-grid Graph.

Fan, Jia Min, 2022. Research on Radioactive Source Search Method based on homogeneous robot formation. SWUST.

Feng, Q., Zhang, C., Lu, J., et al., 2019. Source localization in dynamic indoor environments with natural ventilation: An experimental study of a particle swarm optimization-based multi-robot olfaction method. Build. Environ. 161, 106228.

Feng, Q., Cai, H., Yang, Y., et al., 2020. An experimental and numerical study on a multi-robot source localization method independent of airflow information in dynamic indoor environments. Sustain. Cities Soc. 53, 101897.

Gao, M., Zhang, X., 2022. Cooperative search method for multiple UAVs based on deep reinforcement learning. Sensors 22. Basel,Switzerland.

Huang, S., Wang, W., 2023. An evolutionary navigation algorithm for multi-robot with priority order. IEEE Access 11, 45222–45232.

Ji, Y., Zhao, Y., Chen, B., et al., 2022. Source searching in unknown obstructed environments through source estimation, target determination, and path planning. Build. Environ. 221, 109266.

Jiang, Y.F., 2009. Warning about the source jam incident of irradiation equipment in Qixian County, Henan Province. Nucl. Saf. (4), 16–19.

Li, J., Du, J., 2018. Robust adaptive formation control of underactuated autonomous underwater vehicles under input saturation. In: 2018 Chinese Control and Decision Conference(CCDC), pp. 5798–5803.

Ling, M., Huo, J., Moiseev, G., et al., 2022. Multi-robot collaborative radioactive source search based on particle fusion and adaptive step size. Ann. Nucl. Energy 173.

Liu, H., Wang, Y., Lewis, F.L., 2019. Robust distributed formation controller design for a group of unmanned underwater vehicles. IEEE Transactions on Systems, Man, and Cybernetics: Systems 51, 1215–1223.

McMahon, J., Plaku, E., 2021. Dynamic multi-goal motion planning with range constraints for autonomous underwater vehicles following surface vehicles. In: 2021 IEEE 17th International Conference on Automation Science and Engineering(CASE), vol. 704, p. 711.

McMahon, J., Plaku, E., 2023. Autonomous data collection with dynamic goals and communication constraints for marine vehicles. IEEE Trans. Autom. Sci. Eng. 20, 1607–1620.

Park, M., Oh, H., 2020. Cooperative information-driven source search and estimation for multiple agents. Inf. Fusion 54, 72–84.

Poor, H.V., 2015. An introduction to signal detection and estimation(Adapted from a one-semester graduate course taught at the University of Illinois). springer texts in electrical engineering ume 333 (1), 127–139.

Queralta, Jorge Pena, et al., 2020. Collaborative Multi-robot systems for search and rescue: Coordination and perception arXiv preprint arXiv:2008.12610.

Rahbar, F., Martinoli, A., 2020. A distributed source term estimation algorithm for multi-robot systems. IEEE.

Ristic, B., 2008. Gunatilaka A.Information driven localization of a radiological point source. Inf. Fusion 9 (2), 317–326.

Ristic, B., Gilliam, C., Moran, W., et al., 2020. Decentralized multi-platform search for a hazardous source in a turbulent flow. Inf. Fusion 58, 13–23.

Saha, D., Pattanayak, D., Mandal, P.S., 2022. Surveillance of uneven surface With self-organizing unmanned aerial vehicles. IEEE 21, 1449–1462.

Song, C., He, Y., Ristic, B., et al., 2020. Collaborative infotaxis: searching for a signal-emitting source based on particle filter and Gaussian fitting. Robot. Autonom. Syst. 125, 103414.

Steiner, Jake A., Bourne, Joseph R., et al., 2019. Chemical-source localization using a swarm of decentralized unmanned aerial vehicles for urban/suburban environments. Dynamic Systems and Control Conference DSCC2019-9099, V003T21A006, p. 8.

VasiljevićG, PetrovićT., Arbanas, B., et al., 2020. Dynamic median consensus for marine multi-robot systems using acoustic communication. IEEE Rob. Autom. Lett. 5, 5299–5306.

Wang, S., Chen, L., Gu, D., et al., 2014. Cooperative localization of AUVs using moving horizon estimation. IEEE/CAA Journal of Automatica Sinica 1, 68–76.

Wang, J., Cao, J., Jiang, S., 2017. Fault-tolerant pattern formation by multiple robots: a learning approach. In: 2017 IEEE 36th Symposium on Reliable Distributed Systems (SRDS), pp. 268–269.

Wang, W., Wang, L., Wu, J., et al., 2022. Oracle-guided deep reinforcement learning for large-scale multi-UAVs flocking and navigation. IEEE Trans. Veh. Technol. 71, 10280–10292.

Wei, H., Shen, C., Shi, Y., 2021. Distributed lyapunov-based model predictive formation tracking control for autonomous underwater vehicles subject to disturbances. IEEE Transactions on Systems, Man, and Cybernetics: Systems 51, 5198–5208.

Wiedemann, T., Shutin, D., Lilienthal, A.J., 2019. Model-based gas source localization strategy for a cooperative multi-robot system—a probabilistic approach and experimental validation incorporating physical knowledge and model uncertainties. Robot. Autonom. Syst. 118, 66–79.

Wu, Jun Cheng, 2021. Research on multi-robot formation for nuclear radiation source localization. SWUST.

Xu, J., Huang, F., Wu, D., et al., 2021. Deep reinforcement learning-based multi-AUVs cooperative decision-making for attack-defense confrontation missions. Ocean Engineering.

Xu, X., Meng, W., Cai, Q., et al., 2023. Multiagent coverage search based on Voronoi and sparse heteroscedastic Gaussian process. Asian J. Control 25 (2), 989–1004.

Yan, Z., Liu, Y., Yu, C., et al., 2017. Leader-following coordination of multiple UUV formations under two independent topologies and time-varying delays. J. Cent. S. Univ. 24, 382–393.

Yue, L., Yang, R., Zuo, J., et al., 2022. Unmanned aerial vehicle swarm cooperative decision-making for sead mission: a hierarchical multiagent reinforcement learning approach. IEEE Access 10, 92177–92191.

Zhang, T., Xiao, J., Li, L., et al., 2021. Toward coordination control of multiple fish-like robots: real-time vision-based pose estimation and tracking via deep neural networks. IEEE/CAA Journal of Automatica Sinica 8, 1964–1976.

Zhao, Z., Zhu, B., Zhou, Y., et al., 2023. Cooperative path planning of multiple unmanned surface vehicles for search and coverage task. Drones(Basel) 7 (1), 21.